J. Phys. B: At. Mol. Opt. Phys. **35** (2002) L229–L235 PII: S0953-4075(02)34382-7

LETTER TO THE EDITOR

Must saddle point electrons always ride on the saddle?

F Afaneh[1,2], R Dörner[1], L Schmidt[1], Th Weber[1], K E Stiebing[1], O Jagutzki[1] and H Schmidt-Böcking[1]

[1] Institut für Kernphysik, August-Euler-Straße 6, 60486 Frankfurt am Main, Germany
[2] Department of Physics, Hashemite University, PO Box 150459, Zarqa 13115, Jordan

E-mail: afanehf@yahoo.com

Received 26 February 2002, in final form 17 April 2002
Published 24 May 2002
Online at stacks.iop.org/JPhysB/35/L229

Abstract
The transfer ionization of He and H_2 by incident He^{2+} was investigated at 0.81 au impact velocity employing cold target recoil ion momentum spectroscopy. In addition to electrons in the saddle point region between the target and projectile forming two 'jets' separated by a valley along the projectile beam axis, we find a new group of electrons moving with a velocity greater than the projectile velocity. These new fast forward electrons result from a narrow range of impact parameters and contribute up to 40% to the total cross section of the transfer ionization process.

Slow ion–atom collisions are central to plasma physics, the physics of interstellar media and provide the link from collision physics to chemical reactions. In slow collisions electrons have time to adjust adiabatically to the slowly changing two-centre potential of the target and projectile forming an intermediate quasi-molecule. On rupture of this quasi-molecule the electrons, in most cases, relax into bound states of either the target or the projectile.

In a few cases, however, one electron is promoted to the continuum, leading to ionization. The mechanisms leading to this ejection of electrons are still controversial. Based on classical mechanics Olson *et al* [1] have suggested that electrons which are located on the top of the barrier of the internuclear potential can be left 'stranded' on this potential saddle as the projectile leaves (saddle point mechanism). The qualitative idea of this mechanism was confirmed within the quasimolecular hidden crossing theory, where a series of transitions between quasimolecular states promoting a molecularized electron into the continuum were identified [2–4]. More recently, solutions of the time-dependent Schrödinger equation illustrated the details of the complicated evolution of the electron cloud finally leading to continuum electrons [5, 6]. The CTMC investigation of the role of the saddle point promotion in the slow collisions presented in [6] has suggested that only a small fraction of the continuum electrons released in p on H collisions at 1 au velocity originates from the saddle point ionization mechanism. This result does not agree with the conclusions drawn from the hidden crossing theory [2–4]. The relationships between these rivalling theoretical approaches remain to be clarified.

Experimental images of the velocity distribution of such continuum electrons unveiled a rich structure in the saddle region between the target and projectile velocity [7–9]. In most cases a two-fingered structure in the scattering plane of the projectile with a minimum on the saddle was found. All experimental and theoretical studies so far, however, have concentrated on the region of velocities between the target and projectile, i.e. in the vicinity of the saddle. In this letter we present the discovery of a new structure in the electron continuum well in front of the projectile which in some cases yields an even higher peak than the one in the much-discussed saddle region. These fast forward electrons have been overlooked in all experiments so far due to experimental limitations and are not discussed in the theoretical literature at all.

The experiment was carried out at the electron cyclotron resonance ion source (ECRIS) installed at the Institut für Kernphysik (IKF) in Frankfurt using cold target recoil ion momentum spectroscopy (COLTRIMS) [8, 10]. The ion beam (Z-axis) collided with a well localized and internally cold gas target (Y-axis) provided by a supersonic gas target. An electric field (X-axis) of 13 V mm^{-1} perpendicular to both the ion beam and the gas jet was used to extract the recoil ions and slow ejected electrons in the opposite directions. The electrons were accelerated by this field a distance of 15 mm, then drifted a distance of 40 mm to be detected by a position-sensitive detector of 50 mm diameter. The recoil ions were accelerated in the opposite direction through a distance of 35 mm and then drifted a distance of 128 mm to be detected by a multi-hit position-sensitive detector of 50 mm diameter. The time-of-flight of the electron was about 11 ns and had a small spread of only about 2.5 ns. This allowed us to use the electron time signal as a start for the time-to-amplitude converter (TAC) which was stopped by the recoil time signal. The measured time-of-flight of recoil ions was used in calculating one of the momentum components of the recoil ions. The other two components were calculated from the position on the detector. Two of the three momentum components of the electrons were calculated from the electron position on the electron detector assuming a constant time-of-flight. The resolution achieved in electron velocity distributions is limited by the width of the projectile beam (1 mm) in the Y-direction, the width of the target gas jet (1.1 mm) in the Z-direction, and the lack of a direct measurement of the electron flight time. The resolutions in $V_{\mathrm{e},y}$ and in $V_{\mathrm{e},z}$ are approximately 0.06 and 0.15 au, respectively.

We have investigated the following transfer ionization reactions:

$$\mathrm{He}^{2+} + \mathrm{He} \rightarrow \mathrm{He}^{+} + \mathrm{He}^{2+} + \mathrm{e}^{-} \quad (1)$$

$$\mathrm{He}^{2+} + \mathrm{H}_2 \rightarrow \mathrm{He}^{+} + \mathrm{H}^{+} + \mathrm{H}^{+} + \mathrm{e}^{-}. \quad (2)$$

In reaction (2), the removal of the two electrons from H_2 leads automatically to the dissociation of the molecule and then to the subsequent Coulomb explosion of the remaining two protons. The momentum vector of both protons has been measured. The momentum from this fragmentation process ($P_{\mathrm{H}}^{+} \approx 34$ au) strongly dominates after the typical momentum exchange with the projectile of $P < 8.0$ au. Another process which is sometimes confused with transfer ionization is autoionizing double capture (ADC), i.e.

$$\begin{aligned}\mathrm{He}^{2+} + \mathrm{He}(\mathrm{H}_2) &\rightarrow \mathrm{He}^{0**}(2l2l') + \mathrm{He}^{2+}(2\mathrm{H}^{+}) \\ &\rightarrow \mathrm{He}^{+}(1s) + \mathrm{e}^{-} + \mathrm{He}^{2+}(2\mathrm{H}^{+}). \quad (3)\end{aligned}$$

In this reaction the emitted electron has a well defined energy of about 35 eV (i.e. a momentum of about 1.6 au) in the moving frame but in the laboratory frame it has an angular-dependent energy. The final charge balance is equivalent to a 'pure' transfer ionization one but the primary mechanism is very different (in fact, a double capture process). These electrons are clearly separated from the main part of the electron momentum distribution of the transfer ionization which is produced by the saddle point promotion.

The scattering plane used to present the electron momentum distributions is defined by the beam direction and the recoil momentum vector in reaction (1) or the momentum vector of the centre-of-mass (CM) of both fragments in reaction (2). Distributions of the electron momentum are generated for two special recoil planes; the nuclear scattering plane and the plane perpendicular to the transversal momentum of the projectile. The former plane produced a 'top view' of the electron momentum distribution. The latter plane produced a 'side view' of the electron momentum distribution. In all top-view figures, the recoil ion or the CM of both fragments moves down ($-y$-axis) after the collision.

Electron momentum distributions for side and top views are given in figures 1(a) and (c) for reaction (1) and in (b) and (d) for reaction (2). Note that all horizontal and vertical scales are given in units of the projectile velocity V_p to ease comparison. In both collision systems, the electrons are seen to be preferentially emitted in the forward direction. The salient feature of the electron momentum distributions for both systems consists of the appearance of two groups of electrons with different structures. The first group consists of electrons emitted with velocities between zero and V_p; the vicinity of the saddle point velocity. This group is well known from earlier studies [2, 8, 9, 11]. The other group, seen here for the first time, consists of electrons ejected with velocity greater than the projectile velocity. This group is referred to as the fast forward electrons.

The so-called saddle point electrons are confined to the scattering plane as shown in the side-view distributions for both collision systems. The top-view distributions show that these electrons are emitted in two jets orientated in the scattering plane in the forward direction and off the projectile-axis. This structure is apparent for both collision systems. This structure can be seen more clearly by making a projection of a slice of the two-dimensional distribution near $V_{e,z}/V_p = 0.5$ onto the vertical axis ($V_{e,y}$). Such a projection of figure 1(c) is shown in (g). A similar projection of figure 1(d) is given in (h). Taking into consideration the fact that each of these figures shows only a projection of a slice of the two-dimensional distribution around the saddle point in the saddle vicinity, therefore, these figures do not include any information on the fast forward electrons. It is interesting to note, however, that while for He^{2+} on He more electrons follow the recoil ion, for He^{2+} on H_2 more electrons are emitted away from the CM direction. It has previously been suggested [4, 8, 12] that this structure springs from target ionization along the promoted 2pπ molecular orbital. The process begins with rotational coupling of the 2pσ orbital occupied by the incoming active electron into a 2pπ state at small internuclear distances. The 2pπ orbital is then eventually promoted into the continuum via a series of radial crossings (the so-called $\boldsymbol{T}$-process), keeping the π character. The nodal line along the internuclear axis is a signature of that character.

The fast forward electrons possess a different structure than the saddle point electrons. These electrons reveal a substantial amount of out-of-plane scattering as shown in the side-view distributions; see figures 1(a) and (b). The top-view distributions (figures 1(c) and (d)) show that the fast forward electrons are emitted opposite to the scattered projectile. To further explore these fast forward electrons, the two-dimensional electron momentum distributions in figures 1(c) and (d) are projected onto the beam ($V_{e,z}$) axis. The projections are given in figures 1(e) and (f) respectively. These figures show that the fast forward electrons reveal a distinct peak and yield a significant contribution to the transfer ionization cross section. It is surprising to see that the distribution exhibits a dip at the projectile velocity where, in fast collisions, the cusp electrons are found.

It is illustrative to compare the findings of fast forward electrons reported here for the transfer ionization process with momentum distributions for the single ionization channel. For the latter we find no fast forward electrons, but backward electrons for close impact parameters. This is in agreement with the findings by Abdallah *et al* for the single ionization

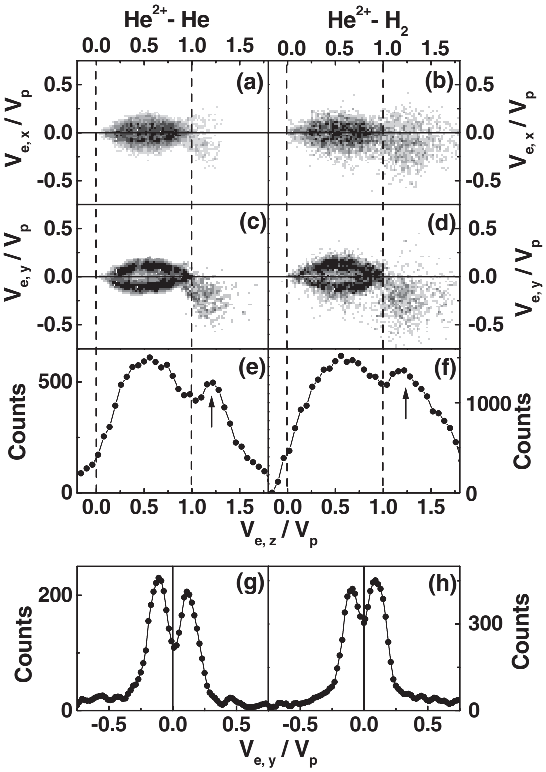

Figure 1. (a) and (b) present side views of the emitted electron momentum distributions in the collision $V_p = 0.81$ au He^{2+} on He and on H_2, respectively. (c) and (d) show the top views of the emitted electron momentum distributions for the previous collision systems. The density scale used in these figures is linear. The intensity of each cell is proportional to the number of counts in that cell. Each image has been normalized so its maximum intensity is near ten units on this scale. The electron velocity components $V_{e,y}$ and $V_{e,z}$ are scaled by the projectile velocity. (e) and (f) show the projections of (c) and (d) on the horizontal axis ($V_{e,z}$). The arrows in both figures point to the fast forward electron group. (g) and (h) show the projections of (c) and (d) near $V_{e,z}/V_p = 0.5$ on the vertical axis ($V_{e,y}$).

of He by He^+ and He^{2+} [9] and for the single ionization of Ne by Ne^+ [13]. They reported a number of electrons in the scattering plane that exhibit a considerable degree of backscattering ($V_{e,z} < 0$). Since in single ionization and transfer ionization the final state of the projectile and target is interchanged, backward electrons and the present fast forward electrons might have a common origin. One might speculate that electrons which are promoted on the saddle for some time during the collision could finally swing around either the target or the projectile by 130° into the backward or forward direction. Which direction is more favourable depends on the gradient of the potential, which is larger for a screened than for a bare Coulomb potential. This speculation is based on the idea that the transfer and ionization processes occur sequentially in that order. Such an idea would be supported by the success of the classical over-barrier model for multiple-electron capture [14]. Based on the fact that the fast forward electrons are observed for He and H_2 target we conclude that they do not originate from electron correlation in the transfer ionization channel, since the correlation in the initial state as well as the details of the potential curves are quite different for the two targets. This supports an independent-electron picture and a mechanism which is more projectile than target dependent. An obvious

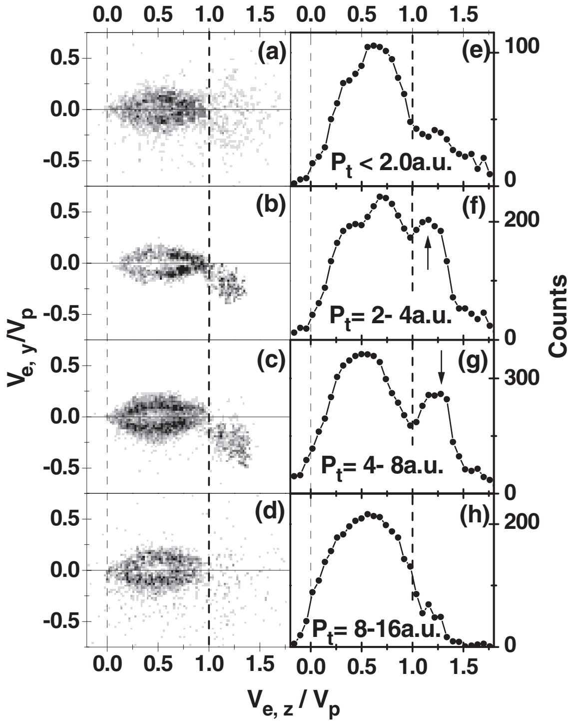

Figure 2. (a)–(d) Top view of the ejected electron momentum in the collision $V_p = 0.81$ au He^{2+} on He for different transverse momentum transfer, i.e. impact parameters ((a) $b > 2.48$ au, (b) $b = 1.24$–2.48 au, (c) $b = 0.62$–1.24 au and (d) $b = 0.31$–0.62 au). (e) and (h) show the projections of (a) and (d) on the horizontal axis ($V_{e,z}$). The arrows point to the fast forward electrons group.

indication of the existence of the fast forward electrons could be seen in the theoretical work of Sidky *et al* [6] figure 1 and [5] figure 3. They found, in classical calculations, as well as in using their two-centre momentum space discretization (TCMSD) method [5], a significant emission of fast forward electrons ($V_{e,z} > V_p$). They provided a classification of ejected electrons into saddle electrons and kinetic electrons. This classification is consistent with the conclusions presented in this study. Also, similar behaviour has been seen by Hagmann *et al* [15] for the multiple ionization of He by incident F^{9+} and I^{23+}, but at high projectile velocities. They measured the doubly differential cross sections (DDCS) for electron emission for the single and multiple ionization of He. They noticed a significantly increased directionality of electron emission in the DDCS in the forward direction, i.e. a large amount of electrons moving with the projectile velocity or even beyond.

To study the impact parameter dependence of the emitted electron momentum distribution in the scattering plane for both collision systems, the electron distribution was gated on different ranges of transverse momentum transfer, i.e. for different ranges of impact parameters ($P < 16$ au, $b > 0.3$ au). The results are shown in figure 2 for reaction (1) and in figure 3 for reaction (2). In these figures the transverse momentum transfer increases from (a) to (d) in figure 2 and from (a) to (c) in figure 3, therefore the impact parameter decreases the same way. These results represent the first experimental study of the impact parameter dependence of the continuum electron momentum distribution in the scattering plane for a molecular target. In

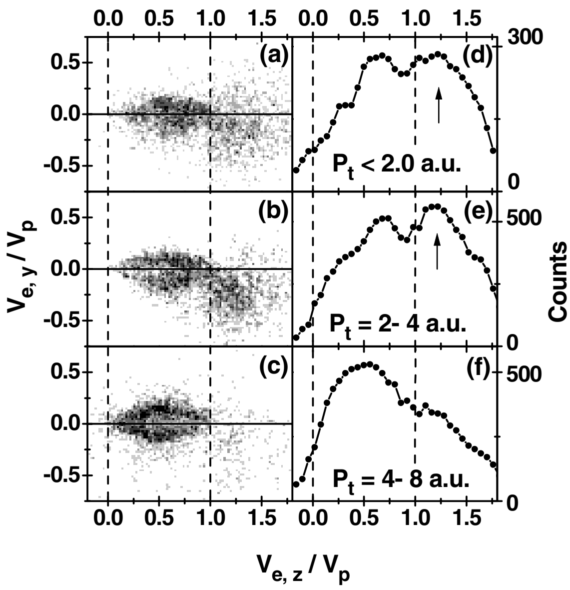

Figure 3. (a)–(c) Top view of the ejected electron momentum in the collision $V_p = 0.81$ au He^{2+} on H_2 for different transverse momentum transfer, i.e. impact parameters. The transverse momentum transfer increases from (a) to (c) and therefore the impact parameter decreases the same way. (d)–(f) show the projections of (a)–(c) on the horizontal axis ($V_{e,z}$). The arrows point to the fast forward electrons group.

both collision systems, the figures show that the distribution in the vicinity of the saddle point velocity exhibits the two-finger structure for all ranges of impact parameter. The corresponding $V_{e,z}/V_p$ projections from each distribution are given in figures 2(e)–(h) for reaction (1) and in figures 3(d)–(f) for reaction (2). These figures demonstrate the fact that the emission of the fast forward electrons exhibits a strong impact parameter dependence. They maximize at transverse momentum transfer of $P = 2$–4 au which, using a screened potential, corresponds to impact parameters of $b = 1.24$–2.48 au.

In conclusion, we have obtained images of the momentum distributions of the continuum electrons liberated in the transfer ionization in 0.81 au He^{2+} on He and H_2 collisions for fully determined motion of the nuclei. We find a huge presence of electrons moving faster forward than the projectile. At certain impact parameters this distinct peak resulting in the electron longitudinal momentum distribution is even higher than the much discussed electrons in the saddle region. These fast forward electrons have been completely overlooked in all studies of slow ion–atom/molecule collisions so far. While the saddle point electrons exhibit a two-finger structure, the fast forward electrons follow the emitted recoil or the direction of the CM. We find a strong impact parameter dependence of the fast forward electrons in both collision systems.

FA gratefully acknowledges support from the DAAD. ThW is grateful for the financial support of the Graduiertenförderung des Landes Hessen. RD acknowledges support through the Heisenberg Program of the DFG and the Adolf-Messer-Stiftung. We thank RoentDek Handels GmbH for the preparation of the position-sensitive detectors and other technical equipment. This work is supported by DAAD, DFG, BMBF and Graduiertenförderung, Volkswagen Stiftung.

References

[1] Olson R E 1983 *Phys. Rev.* A **27** 1871
[2] Pieksma M, Ovchinnikov S, van Eck J, Westerveld W and Niehaus A 1994 *Phys. Rev. Lett.* **73** 46
[3] Ovchinnikov S Yu and Macek J H 1995 *Phys. Rev. Lett.* **75** 2474
[4] Macek J H and Ovchinnikov S Yu 1998 *Phys. Rev. Lett.* **80** 2298
[5] Sidky Emil Y and Lin C D 1999 *Phys. Rev.* A **60** 377
[6] Sidky Emil Y, Illescas Clara and Lin C D 2000 *Phys. Rev. Lett.* **85** 1634
[7] Kravis S *et al* 1996 *Phys. Rev.* A **54** 1394
[8] Dörner R, Khemliche H, Prior M, Cocke C, Gary J, Olson R, Mergel V, Ullrich J and Schmidt-Böcking H 1996 *Phys. Rev. Lett.* **77** 4520
[9] Abdallah M, Cocke C, Wolff W, Wolf H, Kravis S, Stöckli M and Kamber E 1998 *Phys. Rev. Lett.* **81** 3627
[10] Dörner R, Mergel V, Jagutzki O, Spielberger L, Ullrich J, Moshammer R and Schmidt-Böcking H 2000 *Phys. Rep.* **330** 96
[11] Olson R, Gay T, Berry H, Hale E and Irby V 1987 *Phys. Rev. Lett.* **59** 36
[12] Macek J H 1997 *Nucl. Instrum. Methods* B **124** 191
[13] Abdallah M A, Wolff W, Wolf H E, Cocke C L and Stöckli M 1998 *Phys. Rev.* A **58** 3379
[14] Niehaus A 1986 *J. Phys. B: At. Mol. Phys.* **19** 2925
[15] Hagmann S and Ali I 1999 *Phys. Scr.* T **80** 329